Biomacromolecules

Article

Harmonizing the Intracellular Kinetics toward Effective Gene Delivery Using Cancer Cell-Targeted and Light-Degradable Polyplexes

Benchun Jiang, Hua He, Li Yao, Tong Zhang, Jianping Huo, Wei Sun, and Lichen Yin

Biomacromolecules, **Just Accepted Manuscript** • DOI: 10.1021/acs.biomac.6b01774 • Publication Date (Web): 06 Feb 2017

Harmonizing the Intracellular Kinetics toward Effective Gene Delivery Using Cancer Cell-Targeted and Light-Degradable Polyplexes

Benchun Jiang,[1] Hua He,[2] Li Yao,[3] Tong Zhang,[1] Jianping Huo,[1] Wei Sun,[1,*] Lichen Yin[2,*]

[1]Department of General Surgery, Affiliated Shengjing Hospital, China Medical University, Shenyang 110004, China

[2]Jiangsu Key Laboratory for Carbon-Based Functional Materials and Devices, Institute of Functional Nano and Soft Materials (FUNSOM), Soochow University, Suzhou 215123, China

[3]Department of Nephrology, the First Affiliated Hospital, China Medical University, Shenyang 110001, China

*Correspondence authors:

Email: sunw@sj-hospital.org (W. Sun); Tel: 86-24-96615-31311;

lcyin@suda.edu.cn (L. Yin); Tel: 86-512-65882039

ABSTRACT

The success of non-viral gene delivery is often restricted by the multiple cellular barriers that posed inconsistent requirements for vector design. High molecular weight (MW) and cationic charge density are required for polycations to enable effective gene encapsulation, which however, also lead to high toxicity, restricted intracellular cargo release, and poor serum resistance. We herein developed crosslinked polyethyleneimine (PEI) with built-in UV-responsive domains (NP-PEI) which can effectively condense DNA while rapidly de-crosslink upon light triggers to promote intracellular DNA release and reduce material toxicity. HA coating of the polyplexes further enhanced their serum stability by shielding the surface positive charges, and enabled cancer cell targeting to potentiate the transfection efficiencies. Thus, the polyplexes afforded high transfection efficiencies in serum upon light irradiation, outperforming PEI 25k by 1-2 orders of magnitude. This study therefore provides a useful strategy to overcome the critical barriers against non-viral gene delivery.

Keywords: gene delivery, crosslinked polyethyleneimine (PEI), light responsiveness, DNA release, cytotoxicity

INTRODUCTION

Gene therapy, mediated by the cellular delivery of nucleic acids to promote or rectify specific gene expression, holds great potentials in treating human diseases.[1-5] Compared to viral vectors, non-viral gene vectors feature safe delivery of genetic materials with minimal immunogenicity, oncogenicity, or insertional mutagenesis.[6-8] Despite these desired properties, non-viral vectors typically suffer from notably lower transfection efficiencies than viral vectors, mainly because of the multiple cellular barriers that pose inconsistent requirements for vector design.[9-11]

Polycations represent an important category of non-viral gene vectors, which are capable of condensing the anionic nucleic acids to form polyplexes and facilitating their cellular internalization.[12, 13] For the purpose of better gene condensation, polycations with higher molecular weight (MW) and cationic charge density are usually required, due to their stronger affinity with the anionic nucleic acids.[14] However, such strong binding affinity conversely inhibits the dissociation of genes from the polyplexes in the cytoplasm, thus hurdling effective transfection.[15, 16] Polycations with higher MW and cationic charge density also afford stronger membrane activities to promote the cellular internalization, which at the meantime, lead to higher chemotoxicity and lower stability in serum or buffers.[17-21] The above inconsistencies are also noted for polyethyleneimine (PEI), the most widely used polycation-based gene vector that is capable of mediating effective endosomal escape via its unique “proton sponge” effect.[22-25] Branched PEI 25 kDa (PEI 25k) with high MW is a golden standard transfection reagent, which shows high transfection

efficiency yet notable cytotoxicity due to the irreversible cell membrane disruption.[26] Low-MW PEI (< 2 kDa), comparatively, reveals notably lower cytotoxicity while suffers from low transfection efficiency. Covalent modification of polycations with charge-reducing moieties including saccharides,[27] hydrocarbons,[28, 29] and poly(ethylene glycol) (PEG),[30-32] serves as an effective approach to reduce their toxicities. However, the modified polycations usually suffer from compromised gene delivery efficiencies, as a consequence of reduced gene encapsulation capabilities and membrane activities.[33]

Based on these understandings, we herein developed a facile and effective strategy to harmonize the multiple inconsistencies among the various transfection processes, such that the gene delivery efficiencies would be maximized. In support of such design strategy, crosslinked PEI 600 Da that is amenable to light-triggered de-crosslinking was developed, with the light-responsive 2-nitrophenyl moieties in the crosslinker. We reasoned that the light-responsive, crosslinked PEI (NP-PEI) with sufficiently high MW and cationic charge density would allow effective gene condensation and intracellular delivery. Upon external light triggers at the post-transfection stage, the NP-PEI will be rapidly de-crosslinked such that the intracellular gene release can be facilitated and material toxicity can be reduced (Figure 1). We further coated the NP-PEI polyplexes with hyaluronic acid (HA), a natural anionic polysaccharide, with attempts to reduce the surface cationic charges as well as facilitate the recognition of CD44 over-expressing on cancer cell surfaces (Figure 1). As such, we hypothesized the serum resistance will be enhanced due to

HA-mediated repulsion of serum proteins, and the cytotoxicity of polyplexes will also be diminished due to shielding of cationic charges. Although the cationic charge-dependent membrane activities of polyplexes would be diminished upon HA coating, we reasoned that such loss of membrane activities could be recovered due to the HA-strengthened, CD44-mediated endocytosis,[34, 35] and thus the transfection efficiency in cancer cells should be enhanced rather than decreased. The feasibility of such design strategy was explored for DNA delivery, and the HA-assisted, light-manipulated gene delivery properties were mechanically probed in terms of serum stability, gene condensation, gene release, cancer cell targeting efficiency, intracellular kinetics, transfection efficiency, and cytotoxicity.

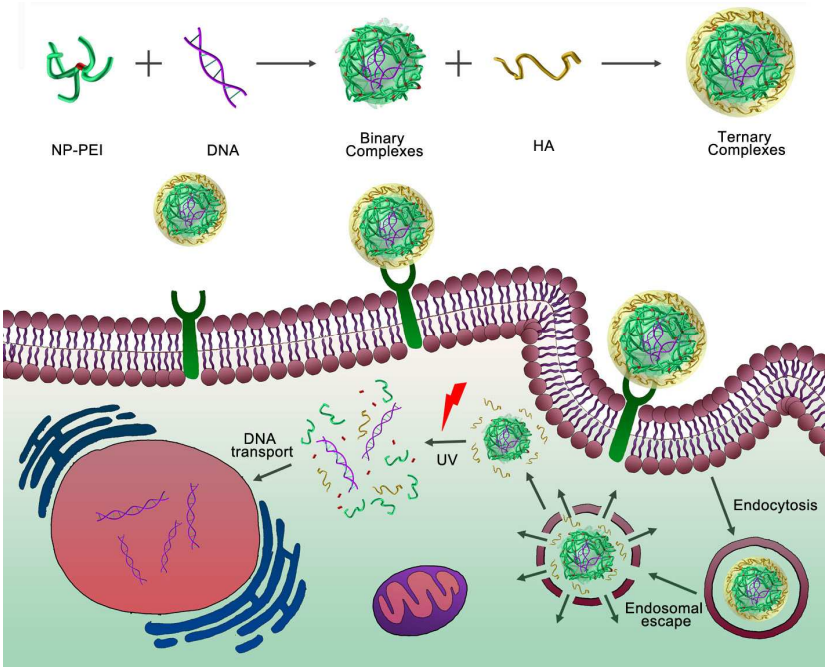

Figure 1. Schematic illustration of cancer cell-targeted, light-enhanced DNA delivery. DNA was condensed by the light-responsive, crosslinked PEI (NP-PEI), which was further coated with HA via electrostatic interaction. The polyplexes were internalized by cancer cells via CD44-mediated endocytosis, followed by endosomal escape via

NP-PEI-assisted "proton sponge" effect. Cytoplasmic DNA release was promoted upon UV light-trigged de-crosslinking of NP-PEI, and DNA was further transported into the nucleic toward gene transcription.

EXPERIMENTAL SECTION

Materials and cell lines. All chemicals were purchased from Sigma-Aldrich (St. Louis, MO, USA) and used as received unless otherwise specified. Anhydrous tetrahydrofuran (THF), dichloromethane (DCM), hexane, and dimethylformamide (DMF) were dried by a column packed with 4Å molecular sieves before use. Pierce BCA assay kit was purchased from Thermo Fisher Scientific (Rockford, IL, USA). Plasmid DNA (pDNA) encoding enhanced luciferase (pLuc) was purchased from Elim Biopharm (Hayward, CA, USA). YOYO-1, Lysotracker Red, and 3-(4,5-dimethylthiahiazol-2-yl)-2,5-diphenyl-2H-tetrazolium bromide (MTT) were purchased from Invitrogen (Carlsbad, CA, USA).

HeLa (human cervix adenocarcinoma), B16F10 (mouse melanoma), HepG2 (human hepatocarcinoma), and A549 (human lung carcinoma) cells were purchased from the American Type Culture Collection (Rockville, MD, USA). Cells were cultured in Dulbecco's Modified Eagle Medium (DMEM) (Gibco, Grand Island, NY, USA) containing 10% fetal bovine serum (FBS).

Synthesis of (2-Nitro-1,3-phenylene)bis(methylene) Diacrylate (NPBMD). NPBMD was synthesized as previously described (Supporting Information Scheme S1).[36] Briefly, 1,3-dimethyl-2-nitrobenzene (15.0 g, 0.10 mol) was mixed with NaOH

solution (0.2 M, 800 mL) under stirring at 95 °C. $KMnO_4$ (66 g, 0.418 mol) was slowly added, and the mixture was refluxed for 24 h. After cooling to room temperature, the mixture was filtered and the filtrate was acidified with HCl to pH 1 to obtain compound **1** as white solid (yield 50%). ^{1}H NMR (DMSO-d_6): δ 8.14 (m, 2H, ArH), 7.72 (m, 1H, ArH).

Compound **1** (16.0 g, 76 mmol) was dissolved in anhydrous THF (100 mL) and cooled to 4 °C in an ice bath. Borane (1.0 M in THF, 400 mL) was slowly added by syringe over 1 h under N_2, and the mixture was stirred at room temperature for 48 h. Methanol (40 mL) was added dropwise to the reaction mixture which was further filtered and dried under vacuum. The residue was dissolved in ethyl acetate and washed with saturated NaCl solution (4 × 100 mL). The organic layer was dried over anhydrous $MgSO_4$, and the solvent was removed under vacuum. The crude product was purified by silica gel column chromatography (hexane/ethyl acetate =1/1) to obtain compound **2** (yield 75%). ^{1}H NMR (DMSO-d_6): δ 7.64 (m, 3H, ArH), 5.55 (t, 2H, −O*H*), 4.68 (d, 4H, −CH_2OH).

Compound **2** (7.3 g, 40 mmol) was dissolved in anhydrous DCM (50 mL), and triethylamine (240 mmol) was added dropwise over 1 h under N_2. Acryloyl chloride (10.9 g, 120 mmol) was slowly added into the reaction mixture by syringe at 0 °C. The mixture was stirred for 18 h at room temperature. The solvent was dried under vacuum and the residue was dissolved in ethyl acetate and washed with saturated NaCl solution (3 × 100 mL). The organic layer was dried over anhydrous $MgSO_4$, and the solvent was removed under vacuum. The crude product was purified by silica gel

column chromatography (hexane/ethyl acetate=1/1) to obtain NPBMD as white crystal (yield 72%). ^{1}H NMR (DMSO-d_6): δ 7.65 (m, 3H, ArH), 6.28 (d, 2H, −CH=CH_2), 6.12 (dd, 2H, −CH=CH_2), 5.95 (d, 2H, −CH=CH_2), 5.23 (s, 4H, ArCH_2O−).

Synthesis of (1,3-Phenylene)bis(methylene) Diacrylate (PBMD). PBMD as a nonresponsive analogue of NPBMD was synthesized by following the same method as described above with 1,3-dimethyl-benzene instead of 1,3-dimethyl-2-nitrobenzene as the starting material (Supporting Information Scheme S2). PBMDA was obtained as colorless viscous liquid (yield 50%). ^{1}H NMR (DMSO-d_6): δ 7.36 (m, 3H, ArH), 6.34 (d, 2H, −CH=CH_2), 6.20 (dd, 2H, −CH=CH_2), 5.94 (d, 2H, −CH=CH_2), 5.16 (s, 4H, ArCH_2O−).

Synthesis of Cross-Linked PEI. NP-PEI was synthesized via Michael addition reaction of NPBMD and PEI 600 (Scheme 1). Briefly, PEI 600 (40 mg) and NPBMD (13 mg, molar ratio of acrylate in NPBMD to primary amine in PEI 600= 1:3) were dissolved in anhydrous DCM (3 mL) and heated to 50 °C in a Teflon-lined screw cap vial under N_2. The mixture was stirred in the dark at 50 °C for 24 h, and the obtained polymer was dialyzed against distilled (DI) water (MWCO = 1 kDa) for 3 days before lyopholization. The MW of the polymer was determined by MALDI-TOF (Bruker, ultraflextreme MALDI-TOF/TOF). The non-responsive analogue, PBMD-crosslinked PEI 600 (P-PEI) was synthesized from PBMD and PEI 600 using the same method.

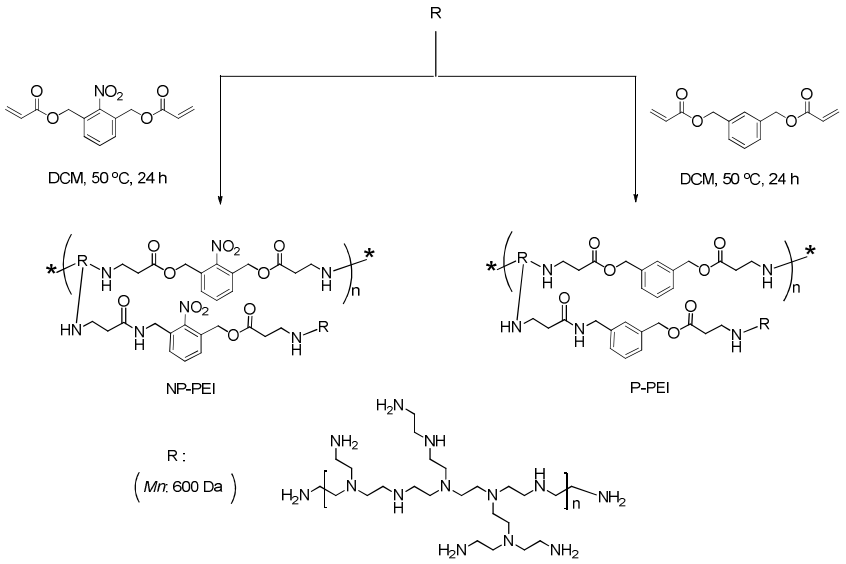

Scheme 1. Synthetic route of NP-PEI and P-PEI.

Preparation and Characterization of Polyplexes. NP-PEI and DNA were separately dissolved in DEPC water at 1 mg/mL. NP-PEI was added to the DNA solution at various weight ratios, and the mixture was vigorously vortexed for 30 s following incubation at RT for 20 min to form the NP-PEI/DNA binary polyplexes. HA (1 mg/mL in DEPC water) was further added to the NP-PEI/DNA polyplexes at various HA/DNA weight ratios. The mixture was incubated at RT for another 1 h to allow surface coating of the binary polyplexes with HA, thus forming the NP-PEI/HA/DNA ternary polyplexes. Freshly prepared polyplexes were subjected to electrophoresis on a 1% agarose gel (100 V, 40 min) to explore the DNA condensation with naked DNA as the control. An ethidium bromide (EB) exclusion assay was further adopted to quantitatively monitor the DNA condensation level. Size and Zeta potential of freshly prepared polyplexes were determined by dynamic laser scanning (DLS) on a Malvern Zetasizer. The stability of polyplexes in salt or serum

was further evaluated by monitoring the particle size alteration of polyplexes following dilution with normal saline (pH 7.2) or DMEM-containing 10% serum for 10 fold and incubation at RT for different time.

Light-Triggered Polyplex Dissociation and DNA Release. Freshly prepared polyplexes were irradiated by UV light (λ=365 nm, 20 mW/cm^2) for different periods of time and incubated at RT for 12 h followed by particle size analysis by DLS. The morphological alteration of polyplexes upon UV irradiation was also observed by transmission electron microscopy (TEM). The DNA condensation level of light-irradiated polyplexes was determined by the gel retardation assay and EB exclusion assay. A heparin replacement assay was further performed to evaluate the light-triggered DNA release from the polyplexes.[36] Briefly, heparin was added to the non-irradiated and the UV-irradiated polyplexes at various final concentrations and the solutions were incubated at 37 °C for 1 h. The DNA condensation level was then quantified using the EB exclusion assay.

In Vitro DNA Transfection. Cells were seeded on 96-well plates at 0.6~1×10^4 cells/well and cultured in serum-containing media for 24 h before reaching 70% confluence. The culture medium was changed to serum-free DMEM or DMEM containing 10% FBS (100 μL/well), and polyplexes were added at 0.3 μg DNA/well. After incubation at 37 °C for 4 h, the medium was replaced by serum-containing DMEM (100 μL/well), and cells were irradiated with UV light (λ=365 nm, 20 mW/cm^2) for different time before further incubation for 20 h. The luciferase activity was then assessed using the Bright-Glo Luciferase assay kit (Promega) and the

cellular protein level was quantified using a BCA kit (Pierce). The transfection efficiency was expressed as relative luminescence unit (RLU) associated with 1 mg of cellular protein (RLU/mg protein).

Intracellular Kinetics. DNA was labeled with YOYO-1 as described previously,[37] and was used to explore the intracellular kinetics of complexes. HeLa cells were seeded on 96-well plates at 1×10^4 cells/well and cultured for 24 h. The medium was changed to opti-MEM and polyplexes were added at 0.3 μg YOYO-1-DNA/well. After incubation at 37 °C for 4 h, cells were washed three times with PBS containing heparin (20 U/mL)[38] and were further lysed with the RIPA lysis buffer (100 μL/well). The YOYO-1-DNA content in the lysate was quantified by spectrofluorimetry (λ_{ex} = 485 nm, λ_{em} = 530 nm) and the protein content was measured using the BCA kit. Uptake level was expressed as ng YOYO-1-DNA associated with 1 mg cellular protein. To explore the HA-mediated targeting effect of polyplexes, cells were pretreated with free HA (10 mg/mL) for 4 h before addition of the polyplexes. The uptake level of YOYO-1-DNA was determined 4 h later as described above.

To explore the internalization pathway of the polyplexes, the cellular uptake study was performed at 4 °C or in the presence of various endocytic inhibitors. Briefly, cells were pre-treated with chlorpromazine (CPZ, 10 μg/mL), genistein (GNT, 100 μg/mL), methyl-β-cyclodextrin (mβCD, 5 mM), wortmannin (WTM, 10 μg/mL), and dynasore (DNS, 80 μM) for 30 min prior to the addition of polyplexes and throughout the 2-h uptake experiment at 37 °C. Results were expressed as percentage uptake

level of control cells that were treated with polyplexes at 37 °C for 2 h in the absence of inhibitors.

The endosomal escape of polyplexes was observed by confocal laser scanning microscopy (CLSM). Briefly, HeLa cells were seeded on chamber slides at 1×10^4 cells/well and were cultured for 24 h before treatment with YOYO-1-DNA-containing polyplexes (1 μg DNA/well) for 4 h. Cells were then washed with cold PBS containing heparin (20 IU/mL) for three times, and the endosomal/lysosomal compartments were stained with Lysotracker Red (100 nM, Invitrogen). After nuclei staining with Hochest33258 (5 μg/mL), cells were observed by CLSM (Zeiss-700, Germany). To further evaluate the UV-triggered intracellular DNA release, rhodamine-labeled NP-PEI (RhB-NP-PEI) and YOYO-1-DNA were used to form polyplexes, which were incubated with HeLa cells for 4 h as described above. Cells were then irradiated with UV light (365 nm, 20 mW/cm^2) for 5 min and further cultured in fresh media for 4 h. The separation of YOYO-1-DNA from RhB-NP-PEI was observed with CLSM following nuclei staining with Hoechst33258, and the colocalization ratio between YOYO-1-DNA and RhB-NP-PEI was quantified as follows using the ImageJ software:[39]

$$\text{Colocalization ratio (\%)} = \frac{\text{YOYO-1 pixels}_{\text{colocalization}}}{\text{YOYO-1 pixels}_{\text{total}}} \times 100$$

Where YOYO-1 pixels$_{\text{colocalization}}$ represents the number of YOYO-1 pixels colocalizing with RhB-NP-PEI and YOYO-1 pixels$_{\text{total}}$ represents the number of all YOYO-1 pixels in the CLSM images. Results were presented as the mean of 20 individual cells.

Cytotoxicity. HeLa cells were seeded on 96-well plates at 1×10^4 cells/well and cultured for 24 h. Cells were then incubated with NP-PEI/DNA (w/w = 2/1), P-PEI/DNA (w/w = 2/1), PEI 25k/DNA (w/w = 1/1), and PEI 600/DNA (w/w = 5/1) polyplexes for 4 h at various polymer final concentrations, irradiated with UV light (365 nm, 20 mW/cm^2) for 5 min, and further cultured in fresh DMEM containing 10% FBS for 20 h. Cells without polyplexes treatment and UV irradiation served as the control. Cell viability was determined by the MTT assay, and results were presented as percentage viability of control cells. In a parallel study, cells were incubated with NP-PEI/HA/DNA polyplexs (w/w/w = 2/2/1) at various DNA amount (0.3, 0.5, 1, and 2 μg/well) for 4 h, irradiated with UV light (365 nm, 20 mW/cm^2) for 5 min, further cultured for 20 h, and subjected to viability assessment using the MTT assay.

Statistical Analysis. Statistical analysis was performed using Student's *t*-test. The differences between test and control groups were judged to be significant at $^*p < 0.05$ and very significant at $^{**}p < 0.01$.

RESULTS AND DISCUSSION

Synthesis of Crosslinked PEI. NP-PEI was synthesized via the Michael addition between the acrylate groups in NPBMD and amine groups in PEI 600. When the acrylate/primary amine molar ratio exceeds 1:3, the reaction mixture got solidified during the 24-h reaction period, which could be possibly due to the excessive crosslinking. Higher temperature than 50 °C and longer reaction time than 24 h would also result in the solidification issue, and thus we fixed the reaction temperature to

50 °C and reaction time to 24 h to prevent solidification. The MW of NP-PEI (acrylate/primary amine molar ratio of 1:3) was determined to be 5478 Da using MALDI-TOF, while after UV irradiation (365 nm, 20 mW/cm^2) for 5 min, its MW decreased to 617 Da, indicating the successful crosslinking of PEI 600 by NPBMD and UV-triggered degradation of NP-PEI.

DNA Condensation and Polyplexes Formation. The capability of NP-PEI to condense DNA was first evaluated using the gel retardation assay. As shown in Figure 2, DNA migration in the 1% agarose gel was retarded at the polymer/DNA weight ratio of 0.5, and was completely restricted to the loading well at the polymer/DNA weight ratio ≥ 1, indicating condensation of DNA by the cationic NP-PEI. Consistent results were obtained from the quantitative EB exclusion assay, wherein more than 80% of the DNA was condensed at the polymer/DNA weight ratio ≥ 1, similar to the PEI 25k as the golden standard (Figure 3A). In comparison, PEI 600 was unable to effectively condense DNA, affording condensation level of ~30% even at high polymer/weight ratio of 10 (Figure 3A). Such discrepancy thus demonstrated that by crosslinking PEI 600 with the NPBMD linker, the DNA condensation capacity could be dramatically improved due to the enhancement of polymer MW. As a result of effective DNA condensation, nano-scale binary polyplexes were formed. As shown in Figure 4A, when the NP-PEI/DNA weight ratio increased, the particle size decreased while the surface charge increased, and polyplexes with diameter of ~130 nm and Zeta potential of ~30 mV were obtained at the polymer/DNA weight ratio ≥ 1.5.

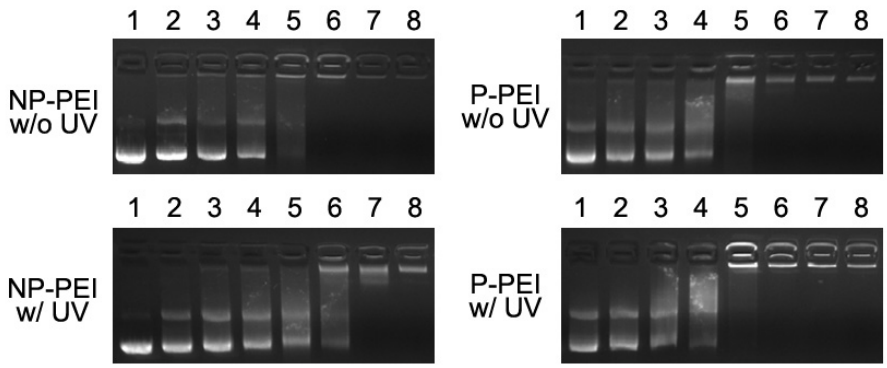

Figure 2. DNA condensation by NP-PEI at various polymer/DNA weight ratios and light-triggered (365 nm, 20 mW/cm^2, 5 min) DNA release as evaluated by the gel retardation assay. The non-responsive P-PEI was incorporated as a control. Lane 1 represents naked DNA; lane 2-8 represents polymer/DNA weight ratios of 0.1, 0.2, 0.3, 0.5, 1, 2, and 5, respectively.

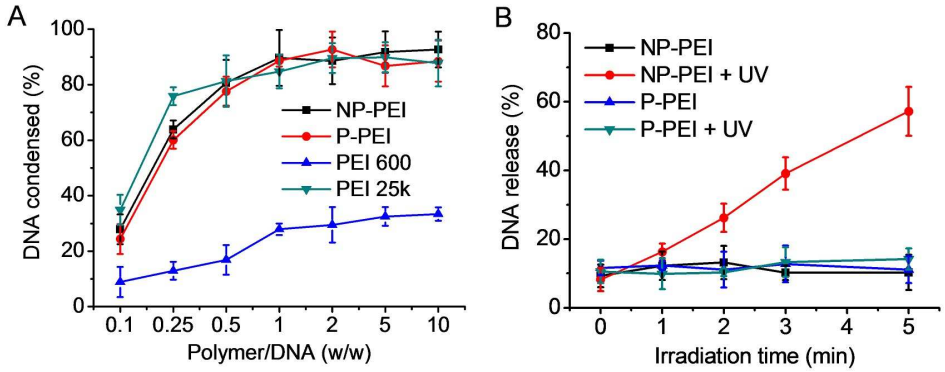

Figure 3. NP-PEI mediates effective DNA condensation while promotes DNA release upon light irradiation. (A) DNA condensation levels of NP-PEI, P-PEI, PEI 25k, and PEI 600 at various polymer/DNA weight ratios as determined by the EB exclusion assay (n=3). (B) DNA release levels of NP-PEI and P-PEI polyplexes (polymer/DNA weight ratio = 2) following UV irradiation (365 nm, 20 mW/cm^2) for different time and further incubation for 12 h (n= 3).

When the binary polyplexes were further coated with HA to form ternary

polyplexes, the particle size did not appreciable change while the Zeta potential decreased when the HA amount was enhanced, indicating the effective coating of the anionic HA onto polyplexes surface that neutralized the cationic charge density (Figure 4C). Particle size slightly increased to ~220 nm at the HA/DNA weight ratio of 2, which could be attributed to the relatively neutral Zeta potential (~-5 mV) that cannot afford sufficient electrostatic repulsions among particles to induce colloidal aggregation.

To further explore the stability of polyplexes, they were diluted with normal saline or DMEM containing 10% FBS for 10 fold. As shown in Figure 4D and Supporting Information Figure S3, particle size of the binary polyplexes dramatically increased upon dilution with salt or serum, while the size of HA-coated ternary polyplexes remained almost un-altered within the 2-h incubation time, indicating that HA coating significantly improved the stability of polyplexes against salt and serum. As an anionic polysaccharide, HA forms a hydrophilic corona on polyplexes surface to reduce the “charge shielding” effect induced by the salt. Additionally, it reduces the electrostatic interactions between polyplexes and serum proteins, and thus prevents adsorption of serum proteins onto polyplexes surfaces that would ultimately lead to particle aggregation.

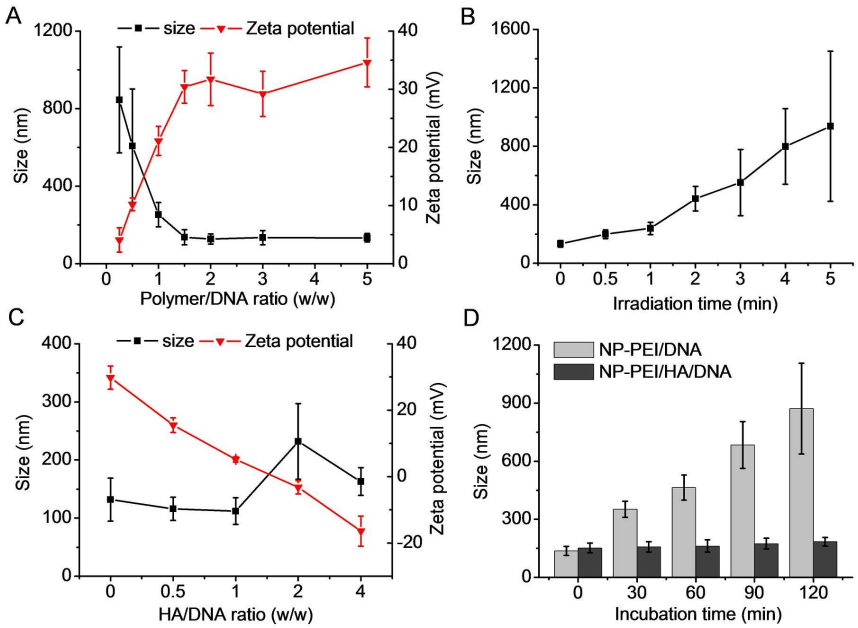

Figure 4. NP-PEI/HA/DNA nanocomplexes afford desired stability and light-induced dissociation. (A) Size and Zeta potential of NP-PEI/DNA polyplexes at various polymer/DNA weight ratios. (B) Alteration of the particle size of NP-PEI/DNA or P-PEI/DNA polyplexes (w/w = 2/1) following UV irradiation (365 nm, 20 mW/cm^2) for different time and further incubation for 12 h. (C) Size and Zeta potential of NP-PEI/HA/DNA polyplexes at various HA/DNA weight ratios. NP-PEI/DNA weight ratio was maintained at 2. (D) Alteration of the particle size of NP-PEI/DNA polyplexes (w/w = 2/1) and NP-PEI/HA/DNA polyplexes (w/w/w = 2/1/1) following dilution with normal saline for 10 fold and incubation for different time.

Light-Triggered DNA Release. The gel retardation assay was first adopted to monitor the UV-induced DNA unpackaging. As shown in Figure 2, NP-PEI completely restricted DNA migration in agarose gel at the polymer/DNA weight ratios of 1 and 2, while after UV irradiation (20 mW/cm^2, 5 min), DNA migration was

observed. In comparison, P-PEI, the non-responsive analogue of NP-PEI, showed negligible alteration in terms of DNA migration after UV irradiation, which verified that light-triggered polymer degradation contributed to the promoted DNA unpackaging. Consistent results were obtained from the quantitative EB exclusion assay, where UV reduced the DNA condensation capacity of NP-PEI but not P-PEI, and longer irradiation time (from 1 to 5 min) accelerated the DNA unpackaging level of NP-PEI (Figure 3B). In accordance with the UV-triggered DNA unpackaging, size of the NP-PEI polyplexes notably enhanced with prolonged UV irradiation time, which could be attributed to the reduced binding affinity of NP-PEI toward DNA that served as the driving force for polyplex formation (Figure 4B). TEM analysis also revealed the morphology alteration of polyplexes from uniformly distributed spheres to the aggregation/dissociation states (Supporting Information Figure S4).

A heparin replacement assay was further utilized to probe the UV-triggered DNA release, which can represent the intracellular DNA release in the presence of anionic polysaccharides/proteins. As shown in Figure 5, 90% of the DNA was released from NP-PEI polyplexes in the presence of 0.25 mg/mL heparin, while upon UV irradiation, a 5-fold lower concentration (0.05 mg/mL) of heparin was required to achieve comparable DNA release level. As the non-responsive control, P-PEI revealed unappreciable alteration in terms of DNA release upon UV irradiation. These findings thus collectively substantiated our design strategy to promote “on-demand” DNA release by mediating instantaneous polymer degradation using external light triggers.

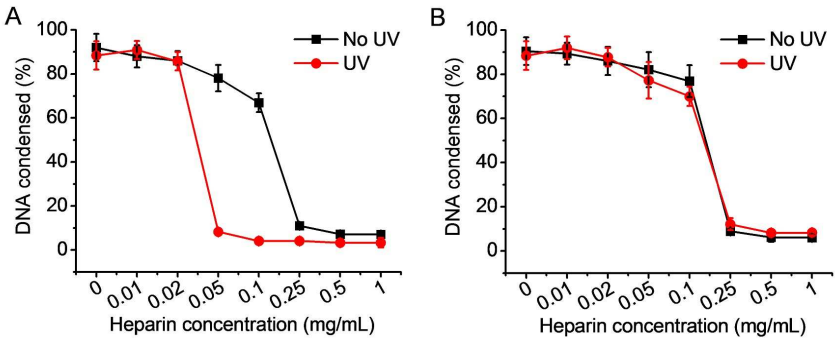

Figure 5. DNA release from NP-PEI/DNA polyplexes (A) and P-PEI/DNA polyplexes (B) in the presence of heparin at various concentrations before and after light irradiation (365 nm, 20 mW/cm^2) for 5 min (n=3).

In Vitro DNA Transfection. NP-PEI with different crosslinking densities was first subjected to transfection studies in HeLa cells in the absence of serum. As shown in Supporting Information Figure S5, NP-PEI 3 exhibited the highest transfection efficiencies at the polymer/DNA weight ratio 2. Thus, NP-PEI 3/DNA (w/w = 2/2) polyplexes were used for further studies, and the nomination of "NP-PEI" was used throughout all studies unless otherwise specified. In a direct comparison, NP-PEI showed slightly higher transfection efficiency than PEI 25k and two orders of magnitude higher efficiency than PEI 600, suggesting that crosslinking of PEI 600 notably enhanced the transfection efficiency by elevating the polymer MW. Upon UV irradiation (20 mW/cm^2, 5 min) at 4 h post polyplexes treatment, the UV-responsive NP-PEI but not the non-responsive P-PEI or PEI 25k, demonstrated significantly enhanced transfection efficiencies, which reached 10-fold higher than PEI 25k as the benchmark positive control (Figure 6A). When the UV irradiation time was prolonged from 1 to 5 min, the transfection efficiency kept increasing (Figure 6B), which

substantiated that UV-triggered polymer degradation potentiated gene transfection by facilitating the intracellular DNA release. When the irradiation time further increased to 10 min, notably decreased transfection efficiency was noted, which could be attributed to the impairment of cell integrity induced by excessive UV irradiation (Supporting Information Figure S6). However, at the laser power of 20 mW/cm^2 and irradiation time of 5 min, unappreciable light toxicity was noted, and the transfection efficiency of P-PEI, PEI 25k, and PEI 600 did not change, indicating that UV irradiation in this proof-of-concept model system did not compromise the cell viability. Considering its efficiency in improving transfection efficiency as well as minimal cytotoxicity, UV irradiation at 20 mW/cm^2 and 5 min was thus adopted for further studies. HA coating of the NP-PEI/DNA polyplexes enhanced the transfection efficiency by several folds under serum-free conditions (Figure 6C), which could be attributed to the promoted cellular internalization as a consequence of HA-mediated cancer cell targeting.

Remarkably compromised transfection efficiency in the presence of serum stands as a critical challenge against polycation-mediated gene transfection. To this regard, we next monitored the transfection efficiencies of polyplexes in HeLa cells in the presence of 10% FBS. As illustrated in Figure 6C, the transfection efficiency of NP-PEI was dramatically decreased by 10 fold in 10% serum compared to that in the serum-free media, which was ascribed to the adsorption of serum protein onto polyplexes surfaces that led to particle aggregation. When HA was coated onto the NP-PEI/DNA binary polyplexes, the transfection efficiency in 10% serum greatly

recovered at the HA/DNA weight ratio of 1. Such results thus highlighted the essential roles of HA coating in enhancing the serum resistance of polyplexes, mainly because HA shielded the surface positive charges and thus reduced the adsorption of serum proteins onto polyplexes surface. When the HA/DNA ratio further increased, the transfection efficiency decreased, presumably due to the alteration of surface charge from positive to negative that prevented the polyplexes from approaching the cell membranes. The generality of HA-assisted, light-enhanced gene transfection was further validated in various cancer cell lines in 10% FBS, including B16F10, HepG2, and A549. As shown in Figure 6D, ternary polyplexes with HA coating outperformed binary polyplexes, and UV irradiation further elevated the transfection efficiencies, leading to the improvement over PEI 25k by 1-2 orders of magnitude. These results therefore collectively substantiated our design strategy to improve cancer cell targeting as well as serum resistance via HA coating and to potentiate gene transfection via light-promoted intracellular DNA release.

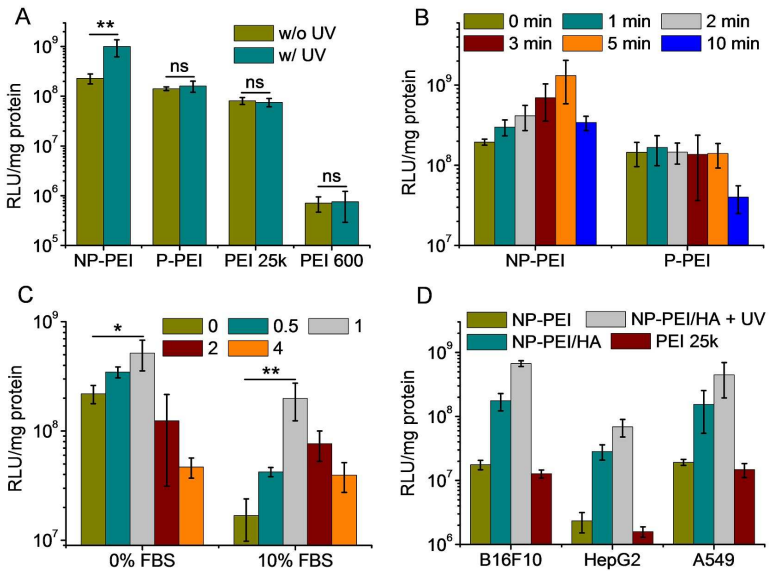

Figure 6. HA-assisted, light-enhanced DNA transfection in cancer cells. (A) Transfection efficiencies of NP-PEI, P-PEI, PEI 25k, and PEI 600 polyplexes (polymer/DNA weight ratios maintained at 2, 2, 1, and 5, respectively) in HeLa cells w/ or w/o UV irradiation (20 mW/cm^2, 5 min) in the absence of serum (n=3). (B) Effect of UV irradiation time (20 mW/cm^2) on the transfection efficiencies of NP-PEI and P-PEI in the absence of serum. Polymer/DNA weight ratios were maintained at 2 (n=3). (C) Transfection efficiencies of NP-PEI/HA/DNA complexes in HeLa cells in the absence or presence of 10% serum at various HA/DNA weight ratios (n=3). NP-PEI/DNA weight ratio was maintained constant at 2. (D) Transfection efficiencies of NK-PEI/DNA (w/w = 2/1), NP-PEI/HA/DNA (w/w/w = 2/1/1), and PEI 25k/DNA (w/w = 1/1) complexes in B16F10, HepG2, and A549 cells in the presence of 10% serum (n=3). Cells were alternatively UV irradiated (20 mW/cm^2) for 5 min post 4-h treatment with NP-PEI/HA/DNA complexes.

Intracellular Kinetics. The transfection efficiencies of gene vectors are predominantly related to their intracellular kinetics. As such, the internalization mechanism as well as the intracellular fate of polyplexes was further explored. Compared to the minimal uptake level of naked DNA, NP-PEI mediated effective cellular uptake of YOYO-1-DNA in HeLa cells, which was slightly higher than PEI 25k (Figure 7A). PEI 600 showed remarkably low DNA uptake level, presumably due to its poor DNA condensation capability. The NP-PEI/HA/DNA ternary polyplexes showed significantly higher uptake level than the NP-PEI/DNA binary polyplexes,

demonstrating that HA coating facilitated cancer cell uptake of polyplexes by binding to the CD44 overexpressing on cancer cell surfaces. Pretreatment of HeLa cells with free HA significantly reduced the cell uptake level of ternary polyplexes but no the binary polyplexes, which further substantiated the HA-mediated targeting effect (Figure 7A).

We then explored the internalization pathway of the polyplexes by performing the cell uptake study at 4 °C or in the presence of various endocytic inhibitors. Energy-dependent endocytosis is blocked at 4 °C; chlorpromazine (CPZ) inhibits clathrin-mediated endocytosis (CME) by triggering the dissociation of the clathrin lattice; genistein (GNT) and mβCD inhibit the caveolae pathway by suppressing tyrosine kinase and depleting cholesterol, respectively; dynasore (DNS) inhibits both CME and caveolae by inhibiting dynamin; wortmannin (WTM) inhibits macropinocytosis by suppressing phosphatidyl inositol-3-phosphate.[38, 39] As shown in Figure 7B, cell uptake was notably decreased by 70~80% at 4 °C, indicating that majority of the polyplexes were internalized via energy-dependent endocytosis. The cell uptake level was also remarkably reduced by CPZ and DNS, while GNT, mβCD, and WTM exerted negligible inhibitory effect, which suggested that polyplexes were mainly internalized via CME but not caveolae or macropinocytosis.

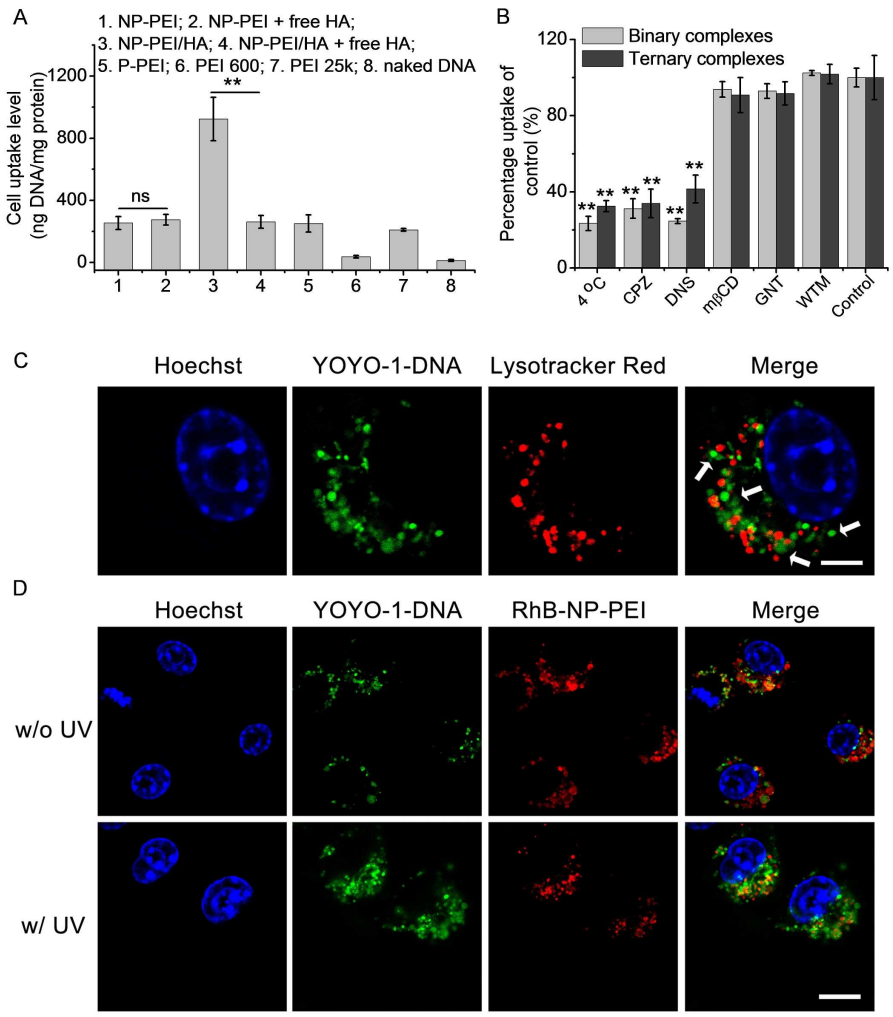

Figure 7. Intracellular kinetics of polyplexes in HeLa cells. (A) Uptake level of NP-PEI/DNA (w/w = 2/1), P-PEI/DNA (w/w = 2/1), NP-PEI/HA/DNA (w/w/w = 2/1/1), PEI 25k/DNA (w/w = 1/1), and PEI 600/DNA (w/w = 5/1) complexes containing YOYO-1-DNA following incubation at 37 °C for 4 h (n = 3). To probe the HA-mediated cancer cell targeting effect, cells were alternatively pre-treated with free HA (10 mg/mL) for 4 h prior to the addition of NP-PEI/DNA or NP-PEI/HA/DNA polyplexes. (B) Uptake level of NP-PEI/DNA (w/w = 2/1) and NP-PEI/HA/DNA (w/w/w = 2/1/1) polyplexes at 4 °C or in the presence of endocytic inhibitors (n=3). (C) CLSM images of HeLa cells following incubation with

NP-PEI/HA/YOYO-1-DNA complexes (w/w/w = 2/1/1) at 37 °C for 4 h (bar = 10 μm). Cell nuclei and endosomes were stained with Hoechst33258 and Lysotracker Red, respectively. White arrows refer to separation between green and red fluorescence. (D) CLSM images of HeLa cells following incubation with RhB-NP-PEI/HA/YOYO-1-DNA complexes (w/w/w = 2/1/1) at 37 °C for 4 h, UV irradiation (20 mW/cm^2) for 5 min, and further incubation for 4 h (bar = 20 μm).

Upon internalization via CME, polyplexes will experience endosomal entrapment, which prevents them from triggering gene transfection unless they can mediate effective endosomal escape. Therefore, we further evaluated the intracellular distribution of NP-PEI ternary polyplexes. CLSM observation revealed extensive internalization of YOYO-1-DNA in HeLa cells post 4-h incubation, and the internalized YOYO-1-DNA (green fluorescence) largely separated from Lysotracker Red-stained endosomes (Figure 7C), suggesting the NP-PEI polyplexes were capable of mediating effective endosomal escape, mainly due to the "proton sponge" effect induced by PEI. To further investigate the UV-triggered DNA release in the cells, we labeled NP-PEI with RhB and observed the co-localization between RhB-NP-PEI and YOYO-1-DNA with CLSM. As shown in Figure 7D, before UV irradiation, red and green fluorescent dots largely overlapped with each other, while after UV irradiation (20 mW/cm^2, 5 min) and further incubation for 4 h, notable separation between two fluorescence signals was clearly noted, and permeated patterns of green fluorescence was observed. In support of such observation, the calculated colocalization ratio between YOYO-1-DNA and RhB-NP-PEI decreased from 82.4 ± 5.6% to 35.7 ±

4.3% upon UV irradiation. These results thus substantiated that light irradiation led to the degradation of NP-PEI and subsequently promoted intracellular DNA release.

Cytotoxicity. Polycations with lower MWs often possess lower cytotoxicities than their high-MW analogues, because they afford fewer contact points with cell membranes and are thus much easier to be expelled from the biological membranes. Based on this understanding, we next evaluated when light-triggered degradation of NP-PEI would diminish its cytotoxicity. To reflect the transfection process, HeLa cells were treated with polyplexes for 4 h, irradiated with UV light (365 nm, 20 mW/cm^2) for 5 min, and further cultured for 20 h before viability assessment using the MTT assay. As depicted in Figure 8A, PEI 25k binary polyplexes exhibited the highest cytotoxicity while PEI 600 showed negligible cytotoxicity even at high concentrations up to 50 μg/mL. NP-PEI and P-PEI polyplexes displayed comparable and concentration-dependent cytotoxicity when UV irradiation was not applied, which was significantly lower than PEI 25k, mainly due to their lower MW than PEI 25k. When cells were UV-irradiated after polyplexes treatment, the cytotoxicity of NP-PEI was greatly alleviated, affording cell viability higher than 90% at 20 μg/mL (Figure 8B). Comparatively, the cytotoxicity of the non-responsive P-PEI, along with PEI 25k and PEI 600, did not change upon UV irradiation, which evidenced that light-triggered polymer degradation greatly reduced the material toxicity. The NP-PEI/HA/DNA ternary polyplexes showed notably lower cytotoxicity than the binary polyplexes especially at high DNA concentrations (Figure 8C), which could be attributed to the shielding of surface positive charges by HA. Consistently, UV

irradiation also decreased the cytotoxicity of NP-PEI/HA/DNA ternary polyplexes, which further demonstrated our proposed design strategy to improve the cell tolerability of NP-PEI via post-transfection light irradiation.

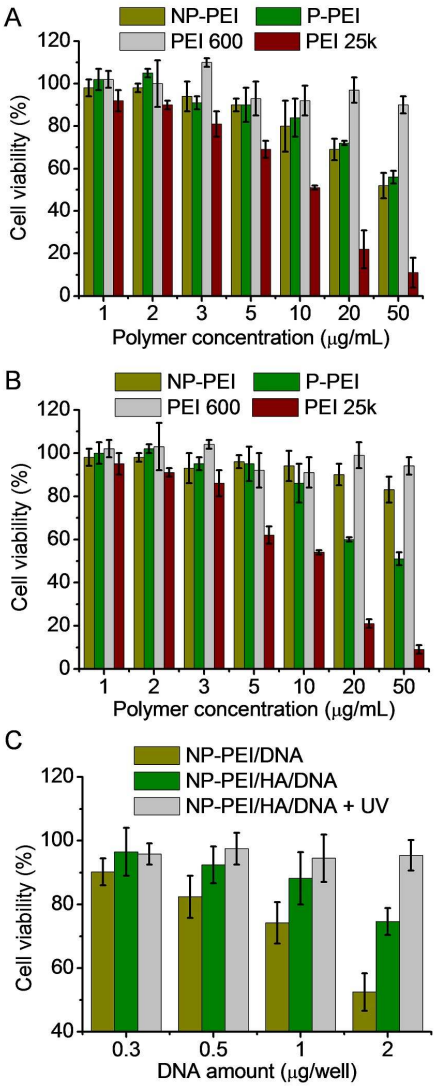

Figure 8. Cytotoxicity of NP-PEI/DNA and P-PEI/DNA polyplexes (w/w = 2/1) in HeLa cells with (A) or without (B) light irradiation (n = 3). Cells were incubated with complexes at various polymer final concentrations for 4 h, irradiated with UV light (365 nm, 20 mW/cm^2) for 5 min, and incubated for 20 h before viability assessment using the MTT assay. (C) Cytotoxicity of NP-PEI/HA/DNA complexes in HeLa cells

following the same treatment as described above (n=3).

CONCLUSIONS

In summary, we developed a strategy to harmonize the inconsistent requirements posed by the multiple cellular processes during gene transfection. Light-degradable, crosslinked PEI was developed to overcome the inconsistency between gene condensation and intracellular gene release, which can undergo instantaneous de-crosslinking upon external light triggers to promote gene unpackaging and diminish the material toxicity at the post-transfection state. HA-coated polyplexes were further developed to overcome the inconsistency between serum resistance and cellular uptake, which enhanced the serum stability via shielding of cationic charges and simultaneously promoted cancer cell uptake via targeting to surface CD44. By synergizing these multiple intracellular responses, the polyplexes developed afforded high transfection efficiencies in serum, remarkably outperforming PEI 25k as the golden standard commercial reagent. This study therefore provides an effective tool in overcoming the multiple cellular barriers against polycation-mediated gene delivery, and renders promising insights into the rational design of non-viral gene vectors. A spectrum of cell types overexpresses CD44 on their cell membranes, such as endothelial cells, embryonic stem cells, and mesenchymal cells, and therefore the HA-promoted gene delivery strategy would find promising extensions to these cells. While UV light suffers from potential mutagenicity and low penetration, it is used here as the external light trigger for the proof-of-concept demonstration of our

designed strategy. To enable higher biocompatibility and deep penetration depth for in vivo use, NIR light-responsive polyplexes are under development.

Supporting Information

Synthetic routes and ^{1}H NMR spectra of monomers, stability of polyplexes, transfection efficiencies of NP-PEI with various crosslinking densities, and cytotoxicity of UV irradiation.

ACKNOWLEDGMENTS

We would like to acknowledge the support from the National Natural Science Foundation of China (51403145 and 51573123), the Science and Technology Department of Jiangsu Province (BK20140333), Natural Science Foundation of Liaoning province (2014021024), Collaborative Innovation Center of Suzhou Nano Science & Technology, and Priority Academic Program Development of Jiangsu Higher Education Institutions (PAPD).

REFERENCES

(1) An, S.; Jiang, X. T.; Shi, J. S.; He, X.; Li, J. F.; Guo, Y. B.; Zhang, Y.; Ma, H. J.; Lu, Y. F.; Jiang, C. *Biomaterials* **2015,** *53*, 330-340.
(2) Li, J. F.; Zhou, L.; Ye, D. Y.; Huang, S. X.; Shao, K.; Huang, R. Q.; Han, L.; Liu, Y.; Liu, S. H.; Ye, L. Y.; Lou, J. N.; Jiang, C. *Adv. Mater.* **2011,** *23*, 4516-4520.
(3) Lu, H.; Wang, D. L.; Kazane, S.; Javahishvili, T.; Tian, F.; Song, F.; Sellers, A.; Barnett, B.; Schultz, P. G. *J. Am. Chem. Soc.* **2013,** *135*, 13885-13891.
(4) Knipe, J. M.; Strong, L. E.; Peppas, N. A. *Biomacromolecules* **2016,** 17, 788-797.
(5) Mangraviti, A.; Tzeng, S. Y.; Kozielski, K. L.; Wang, Y.; Jin, Y. K.; Gullotti, D.; Pedone, M.; Buaron, N.; Liu, A.; Wilson, D. R.; Hansen, S. K.; Rodriguez, F. J.; Gao, G. D.; DiMeco, F.; Brem, H.; Olivi, A.; Tyler, B.; Green, J. J. *ACS Nano* **2015,** *9*,

1236-1249.
(6) Wang, M.; Alberti, K.; Varone, A.; Pouli, D.; Georgakoudi, I.; Xu, Q. B. *Adv. Healthc. Mater.* **2014,** *3*, 1398-1403.
(7) Thomas, C. E.; Ehrhardt, A.; Kay, M. A. *Nat. Rev. Genet.* **2003,** *4*, 346-358.
(8) Davis, M. E.; Zuckerman, J. E.; Choi, C. H. J.; Seligson, D.; Tolcher, A.; Alabi, C. A.; Yen, Y.; Heidel, J. D.; Ribas, A. *Nature* **2010,** *464*, 1067-1070.
(9) Wang, M.; Sun, S.; Alberti, K. A.; Xu, Q. B. *ACS Synth. Biol.* **2012,** *1*, 403-407.
(10) Krivitsky, A.; Polyak, D.; Scomparin, A.; Eliyahu, S.; Ori, A.; Avkin-Nachum, S.; Krivitsky, V.; Satchi-Fainaro, R. *Biomacromolecules* **2016,** *17*, 2787-2800.
(11) He, H.; Bai, Y. G.; Wang, J. H.; Deng, Q. R.; Zhu, L. P.; Meng, F. H.; Zhong, Z. Y.; Yin, L. C. *Biomacromolecules* **2015,** *16*, 1390-1400.
(12) Islam, M. A.; Reesor, E. K. G.; Xu, Y. J.; Zope, H. R.; Zetter, B. R.; Shi, J. J., *Biomater. Sci.* **2015,** *3*, 1519-1533.
(13) deRonde, B. M.; Torres, J. A.; Minter, L. M.; Tew, G. N. *Biomacromolecules* **2015,** *16*, 3172-3179.
(14) Rose, V. L.; Shubber, S.; Sajeesh, S.; Spain, S. G.; Puri, S.; Allen, S.; Lee, D. K.; Winkler, G. S.; Mantovani, G. *Biomacromolecules* **2015,** *16*, 3480-3490.
(15) Tan, X. Y.; Li, B. B.; Lu, X. G.; Jia, F.; Santori, C.; Menon, P.; Li, H.; Zhang, B. H.; Zhao, J. J.; Zhang, K. *J. Am. Chem. Soc.* **2015,** *137*, 6112-6115.
(16) Tan, J. K. Y.; Choi, J. L.; Wei, H.; Schellinger, J. G.; Pun, S. H. *Biomater. Sci.* **2015,** *3*, 112-120.
(17) Mintzer, M. A.; Simanek, E. E. *Chem. Rev.* **2009,** *109*, 259-302.
(18) Ko, I. K.; Ziady, A.; Lu, S.; Kwon, Y. J. *Biomaterials* **2008,** *29*, 3872-81.
(19) Lu, X. G.; Tran, T. H.; Jia, F.; Tan, X. Y.; Davis, S.; Krishnan, S.; Amiji, M. M.; Zhang, K. *J. Am. Chem. Soc.* **2015,** *137*, 12466-12469.
(20) Zheng, N.; Yin, L.; Song, Z.; Ma, L.; Tang, H.; Gabrielson, N. P.; Lu, H.; Cheng, J. *Biomaterials* **2014,** *35*, 1302-14.
(21) Hellmund, M.; Achazi, K.; Neumann, F.; Thota, B. N. S.; Ma, N.; Haag, R. *Biomater. Sci.* **2015,** 3, 1459-1465.
(22) Akinc, A.; Thomas, M.; Klibanov, A. M.; Langer, R. *J. Gene. Med.* **2005,** *7*, 657-663.
(23) Neu, M.; Germershaus, O.; Behe, M.; Kissel, T. *J. Control. Release* **2007,** *124*, 69-80.
(24) Tripathi, S. K.; Gupta, N.; Mahato, M.; Gupta, K. C.; Kumar, P. *Colloids Surf. B Biointerfaces* **2014,** *115*, 79-85.
(25) Yeh, P.-H.; Sun, J.-S.; Wu, H.-C.; Hwang, L.-H.; Wang, T.-W. *RSC Adv.* **2013,** *3*, 12922-12932.
(26) Grabowska, A. M.; Kircheis, R.; Kumari, R.; Clarke, P.; McKenzie, A.; Hughes, J.; Mayne, C.; Desai, A.; Sasso, L.; Watson, S. A.; Alexander, C. *Biomater. Sci.* **2015,** *3*, 1439-1448.
(27) McLendon, P. M.; Fichter, K. M.; Reineke, T. M. *Mol. Pharmaceut.* **2010,** *7*, 738-750.
(28) Oskuee, R. K.; Dehshahri, A.; Shier, W. T.; Ramezani, M. *J. Gene. Med.* **2009,** *11*, 921-932.

(29) Wang, Y.; Li, J.; Chen, Y.; Oupicky, D. *Biomater. Sci.* **2015,** *3*, 1114-1123.
(30) Venkataraman, S.; Ong, W. L.; Ong, Z. Y.; Loo, S. C. J.; Ee, P. L. R.; Yang, Y. Y. *Biomaterials* **2011,** *32*, 2369-2378.
(31) Deshpande, M. C.; Davies, M. C.; Garnett, M. C.; Williams, P. M.; Armitage, D.; Bailey, L.; Vamvakaki, M.; Armes, S. P.; Stolnik, S. *J. Control. Release* **2004,** *97*, 143-156.
(32) Yin, L.; Song, Z.; Kim, K. H.; Zheng, N.; Tang, H.; Lu, H.; Gabrielson, N.; Cheng, J. *Biomaterials* **2013,** *34*, 2340-2349.
(33) Lee, Y.; Miyata, K.; Oba, M.; Ishii, T.; Fukushima, S.; Han, M.; Koyama, H.; Nishiyama, N.; Kataoka, K. *Angew. Chem. Int. Ed.* **2008,** *47*, 5163-5166.
(34) Kim, T. G.; Lee, Y.; Park, T. G. *Int. J. Pharm.* **2010,** *384*, 181-188.
(35) Jiang, G.; Park, K.; Kim, J.; Kim, K. S.; Hahn, S. K. *Mol. Pharm.* **2009,** *6*, 727-737.
(36) Deng, X. J.; Zheng, N.; Song, Z. Y.; Yin, L. C.; Cheng, J. J. *Biomaterials* **2014,** *35*, 5006-5015.
(37) Yin, L. C.; Tang, H. Y.; Kim, K. H.; Zheng, N.; Song, Z. Y.; Gabrielson, N. P.; Lu, H.; Cheng, J. J. *Angew. Chem. Int. Ed.* **2013,** *52*, 9182-9186.
(38) McNaughton, B. R.; Cronican, J. J.; Thompson, D. B.; Liu, D. R. *P. Natl. Acad. Sci. USA* **2009,** *106*, 6111-6116.
(39) He, H.; Zheng, N.; Song, Z. Y.; Kim, K. H.; Yao, C.; Zhang, R. J.; Zhang, C. L.; Huang, Y. H.; Uckun, F. M.; Cheng, J. J.; Zhang, Y. F.; Yin, L. C. *ACS Nano* **2016,** *10*, 1859-1870.

TOC

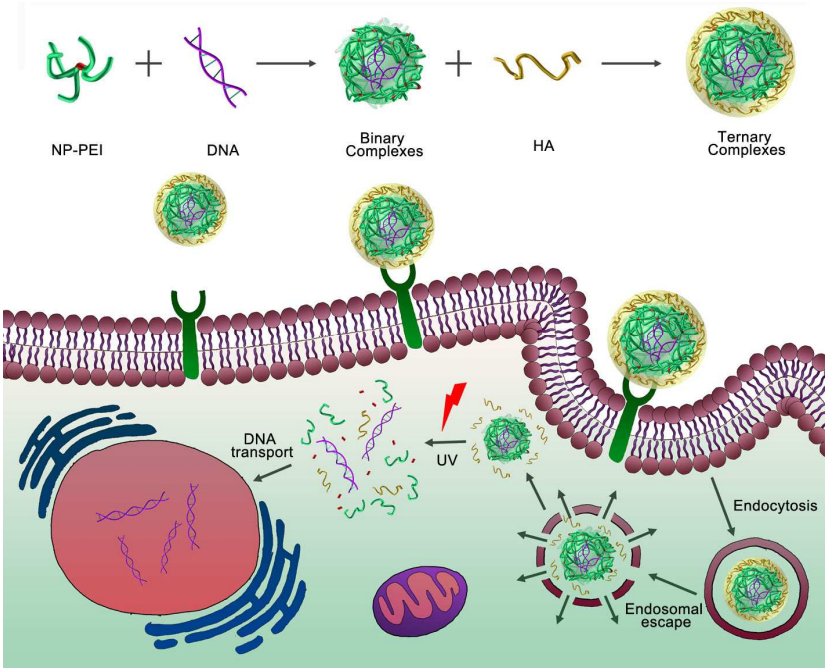
NP-PEI
DNA
Binary Complexes
HA
Ternary Complexes
DNA transport
UV
Endocytosis
Endosomal escape